

Imaging Volcanic Interiors with MT Data

Vjacheslav Spichak

Summary. Three-dimensional (3-D) finite-difference modeling shows the sensitivity of the MT method to the electrical structure of volcanic zones. Modeling is done with the program FDM3D-MT, which allows relief topography, mixed conductivity structures (1-D, 2-D, and 3-D), different layered structures at infinity, and calculation of MT fields at arbitrary levels in the earth and atmosphere.

Numerical experiments with different field components and their transforms—including impedances, apparent resistivities, and magnetic transfer functions—indicate that conductivity gradients in volcanic zones can be identified on plots of isosurfaces of the complex electric field and on isosurfaces of the amplitudes and phases of tensor impedances. The actual conductivity values, however, are constrained poorly.

Interpretation is aided by reduction of the data to an artificial reference plane, positioned in the atmosphere above the top level of the relief surface, followed by the construction of 3-D pseudogeolectrical structure. Examples show the possibility of 3-D imaging of volcanic environments with MT data measured not only at the Earth's surface, but also at different levels in the atmosphere.

1 Introduction

Magnetotelluric (MT) sounding has been used to monitor volcanic activity and to help understand the processes leading to eruptions (Fitterman et al., 1988; Mogi and Nakama, 1990). Modeling of these applications, however, has been relatively crude. For example, Newman et al. (1985) modeled a homogeneous prism in a layered earth with a 3-D integral equation method to study the detectability of a magma chamber, whereas Moroz et al. (1988) built a more elaborate scale model to study the distortion of MT fields by a volcanic cone, but the conductivity of all conductive elements of the structure was equal to 10^6 S/m. I have studied the resolving power of the MT method in volcanic zones with software developed at the Geophysical Research Center in Moscow for use on small computers (Spichak, 1983a, 1985; Zhdanov and Spichak, 1989,1992). This software allows modeling and analysis of MT fields in a general 3-D model of the Earth, including topography at the Earth's surface. After a brief description of the

Geophysical Research Center, Varshavskoe sh.8, Moscow, 113105, Russia.

modeling algorithm, I present some results aimed at determining those components of the natural electromagnetic (EM) fields (and their transforms) that are most sensitive to the internal structure of volcanoes.

2 The 3-D finite-difference algorithm

Let some domain V in the earth be isotropic, nonmagnetic ($\mu = \mu_0$) and characterized by a 3-D distribution of the electrical conductivity $\sigma(x, y, z)$. At the periods used in MT sounding, the field satisfies the quasi-static Maxwellian equations:

$$\nabla \times \mathbf{H} = \sigma \mathbf{E} \quad (1)$$

$$\nabla \times \mathbf{E} = i\omega\mu\mathbf{H} \quad (2)$$

with harmonic time-dependence $\exp(-i\omega t)$. Combining these equations with the identity (take the divergence of the first equation),

$$\sigma \nabla \cdot \mathbf{E} = -(\mathbf{E} \cdot \nabla \sigma)$$

gives the following equation for the electric field:

$$\Delta^2 \mathbf{E} + \nabla(\mathbf{E} \cdot \nabla \sigma / \sigma) + k^2 \mathbf{E} = 0 \quad (3)$$

where $k = (i\omega\mu_0)^{1/2}$, $\text{Re } k > 0$. To determine the EM field in the domain V , first, the partial differential Eq. (3) for the electric field \mathbf{E} is solved; then, the magnetic field \mathbf{H} can be determined from Eq. (2).

Let the continuous vector function \mathbf{E} be replaced by the discrete vector function \mathbf{U} , defined only at the nodes of a rectangular grid. Integrating Eq. (3) over the elementary volume in the vicinity of each node (l, m, n) gives

$$\oint_{S_{l,m,n}} \nabla \mathbf{U}_{l,m,n} ds + \oint_{S_{l,m,n}} (\mathbf{U}_{l,m,n} \cdot \frac{\nabla \sigma_{l,m,n}}{\sigma_{l,m,n}}) ds + \int_{V_{l,m,n}} k_{l,m,n}^2 \mathbf{U}_{l,m,n} dv = 0 \quad (4)$$

($l = 1, 2, \dots, L$; $m = 1, 2, \dots, M$; $n = 1, 2, \dots, N$)

Approximating the derivatives of \mathbf{U} and a in Eq. (4) by finite differences and the integrals by the trapezoid rule gives the linear algebraic equations,

$$\begin{aligned} \mathbf{U}_{l,m,n} = & \hat{D}_{l,m,n}^{(0)-1} (\hat{D}_{l,m,n}^{(1)} \mathbf{U}_{l,m,n-1} + \hat{D}_{l,m,n}^{(2)} \mathbf{U}_{l,m,n} + \hat{D}_{l,m,n}^{(3)} \mathbf{U}_{l-1,m,n} + \\ & \hat{D}_{l,m,n}^{(4)} \mathbf{U}_{l+1,m,n} + \hat{D}_{l,m,n}^{(5)} \mathbf{U}_{l,m+1,n} + \hat{D}_{l,m,n}^{(6)} \mathbf{U}_{l,m,n+1}) \end{aligned} \quad (5)$$

($l = 1, 2, \dots, L$; $m = 1, 2, \dots, M$; $n = 1, 2, \dots, N$), where $\hat{D}^{(i)} = 1, 2, \dots, 6$ are 3×3 matrices determined by the grid geometry, the conductivity distribution, and the frequency.

For boundary conditions at the edges of the modeling domain, the following differential boundary condition is usually accurate, particularly for models with topography at the earth-air interface (Spichak, 1985):

$$(1 - ikr + r \frac{\partial}{\partial r})(\mathbf{E} - \mathbf{E}^n) = 0 \quad (6)$$

where \mathbf{E}^n is a normal electrical field, r is the distance to the points on the boundary of the modeling domain.

The resulting matrix of a system of linear equations has a block-banded shape and is very sparse. To solve it efficiently, a block overrelaxation technique is used:

$$\mathbf{U}^{(t+1)} = (1-\nu)\mathbf{U}^t + \nu\mathbf{U}^{(t+1/2)}, \quad (0 < \nu < 2) \quad (7)$$

where t is a number of the iteration. To minimize the total number of iterations, the relaxation ratio, ν , is automatically corrected during the iterations.

In principle, the magnetic field H can be calculated readily from the electric field by differentiating it using the finite-difference approximation of Eq. (2). In regions with large conductivity contrasts, however, this can generate large errors. In particular, it is practically impossible to correctly determine the horizontal components H_x and H_y at the Earth's surface because of numerical instability in derivatives $\partial E_x/\partial z$ and $\partial E_y/\partial z$.

The horizontal components can be obtained accurately from the vertical component (whose finite-difference computation is stable) by the Hilbert transforms,

$$H_x(x_0, y_0, 0) = H_x^n - (2\pi)^{-1} \iint_S \frac{H_z(x, y, 0)(x - x_0)}{r^3} dx dy \quad (8)$$

$$H_y(x_0, y_0, 0) = H_y^n - (2\pi)^{-1} \iint_S \frac{H_z(x, y, 0)(y - y_0)}{r^3} dx dy, \quad (9)$$

where $r = [(x - x_0)^2 + (y - y_0)^2]^{1/2}$; S is the Earth's surface (restricted in practice by the boundaries of the modeling domain).

The program package FDM3D-MT (Spichak, 1983b), which realizes the above algorithm, runs very efficiently on personal computers (a model with 32 000 grid nodes runs in 30-40 min on a IBM PC AT 486), requires modest core memory, and gives accurate results. The program allows models with a relief topography, mixed type of conductivity structure (1-D, 2-D, or 3-D regions in the same model), different 1-D layering at the boundaries of the model, and calculation of MT fields at arbitrary levels in the earth and atmosphere.

3 Imaging volcanic interiors

3.1 Model of the volcano

To study the MT response in volcanic environments, I used a 3-D geoelectrical model of a typical volcano of Hawaiian type, based on a model constructed in 1989 (with Prof. George Keller) originally to determine whether the MT method could detect internal processes in the Kilauea volcano that had been found in previous EM measurements in this area (Jackson and Keller, 1972).

The model represents a shield volcano, characterized by a low and flat summit formed by homogeneous basaltic rocks (Fig. 1). Its flanks stretch down into the ocean; the conductivity of the ocean water was taken to be 3.6 S/m. The volcano's summit, 0.5-km thick, is formed by basaltic lavas with conductivity $\sigma = 0.001$ S/m. There is a small layer, 0.8-km thick, with conductivity $\sigma = 0.01$ S/m at the boundary between the air and the ocean. Below are porous volcanic lavas, which are characterized by high content of salty water (this zone is 1.7 km thick and has a conductivity $\sigma = 0.17$ S/m). Then, at a 3-km depth from the volcano summit, there are dense lava formations 5.5-km thick with conductivity $\sigma = 0.01$ S/m, underlined by the crystalline crust with conductivity

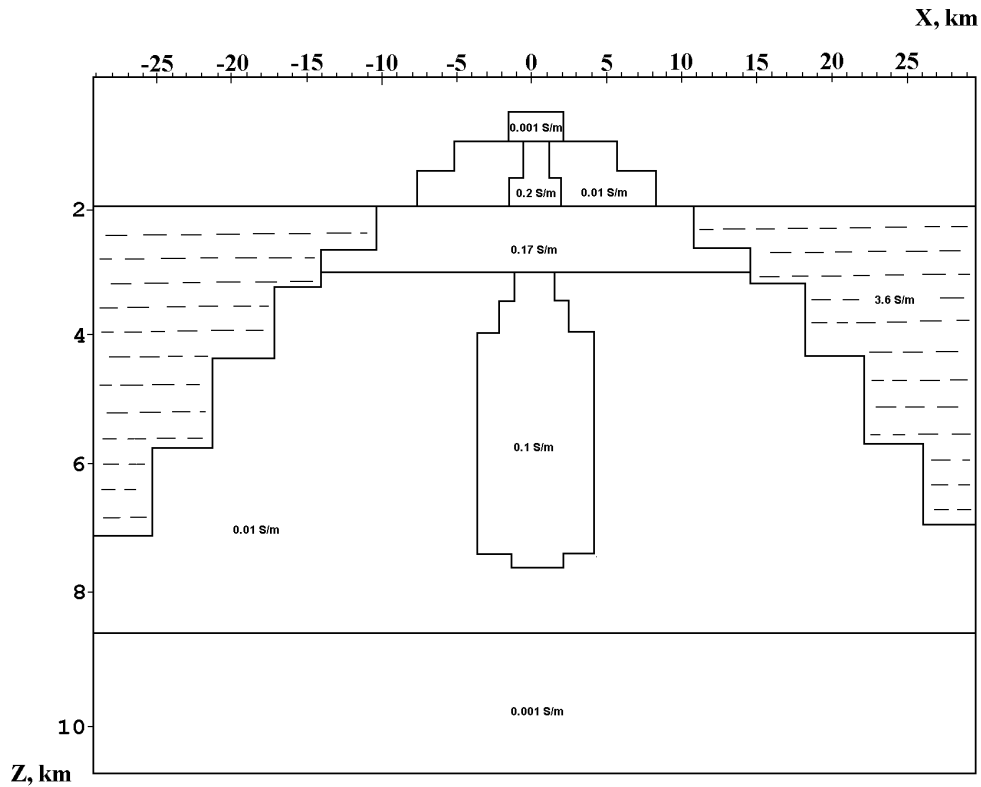


Fig.1. A model of the volcano of Hawaiian type.

$\sigma = 0.001$ S/m. Other details of the geoelectrical structure are not important for this study.

The conductivity distribution in the model was considered to be symmetrical with two vertical planes of symmetry. So, only one-quarter of the 3-D grid was used for calculations.

3.2 Synthetic MT pseudosections

MT fields for this model were synthesized for two polarizations of the primary field at periods $T = 0.1, 1, 10,$ and 100 s. Then, a number of the MT field transformations were calculated and analyzed at different levels in the atmosphere to find those that are most sensitive to the parameters of the model. The analysis used an algorithm for 3-D imaging of geoelectrical structure, which uses transformations of the data recorded at the same level for several periods to create the isosurfaces in the system of coordinates $(X, V, \log_{10} T)$.

For this model, direct estimation of the conductivity distribution from pseudosections of the apparent resistivity is very difficult. In contrast, 3-D isosurfaces or 2-D maps of the isolines of the transforms based on the impedance phases and on the in-phase and quadrature parts of the horizontal electric fields are the best for imaging the complicated geoelectrical structure of the volcano (Figs. 2-5).

In particular, Figs. 2 and 3 show the vertical cross-sections of the volcano overlapped by the maps of isolines of the transformed impedance phases (ϕ_{xy} and ϕ_{det} , correspondingly), constructed for the plane at a height 0.5 km above the summit of the volcano. Although the values attached to the isosurfaces have little to do with the

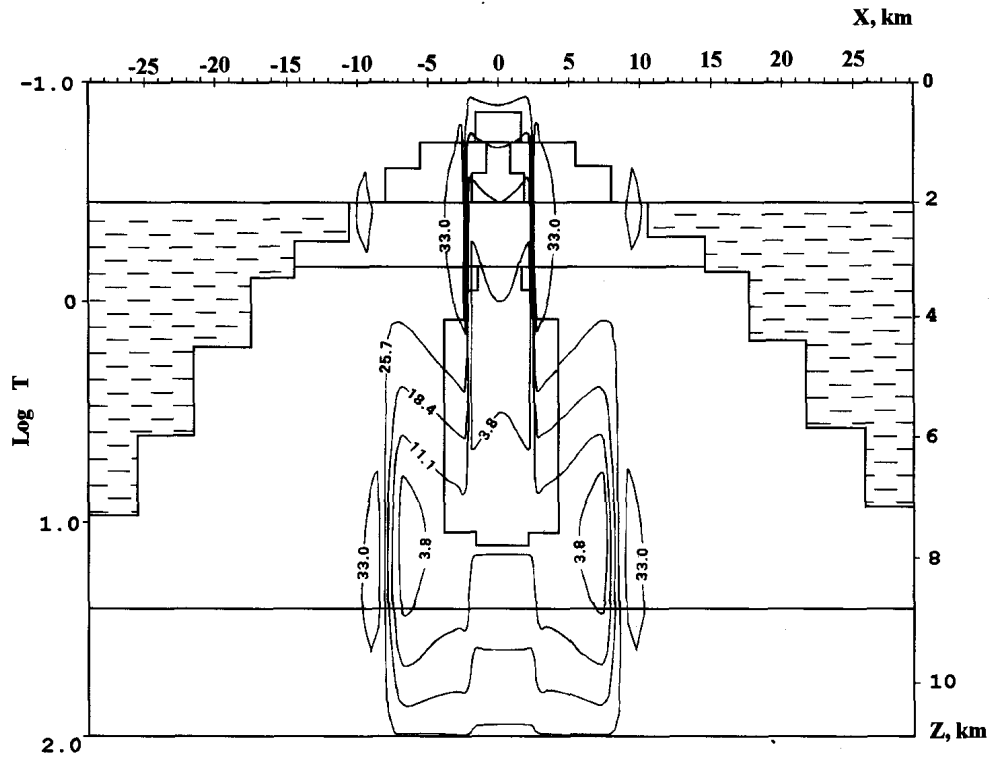


Figure 2. Pseudosection of $\phi_{xy} (\times 10^{-1})$ for volcano model shown in Fig. 1.

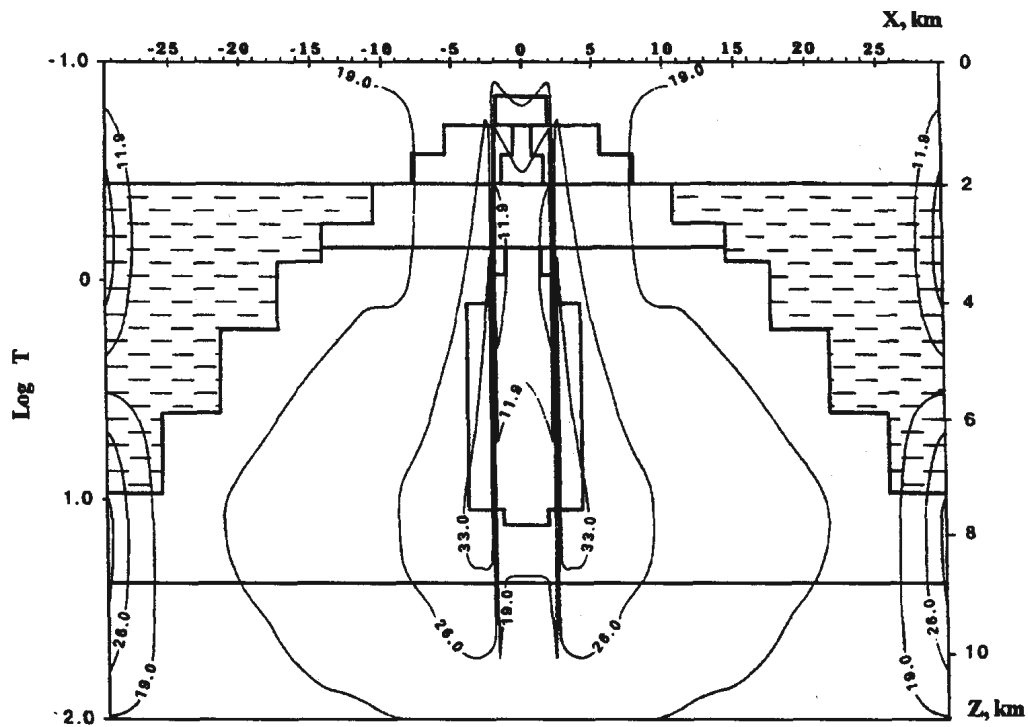


Figure 3. Pseudosection of $\phi_{det} (\times 10^{-1})$ for volcano model shown in Fig. 1.

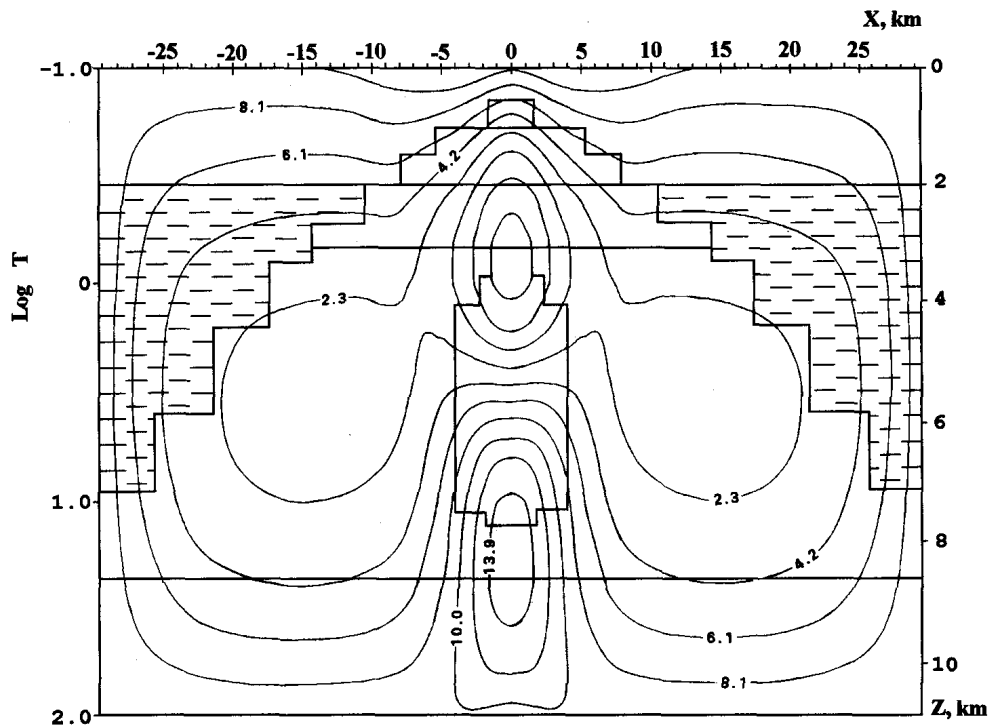


Figure 4. Pseudosection of $\text{Re } E_y$ ($\times 10^1$) for volcano model shown in Fig. 1. Result is based on an incident electrical field, parallel to y-axis.

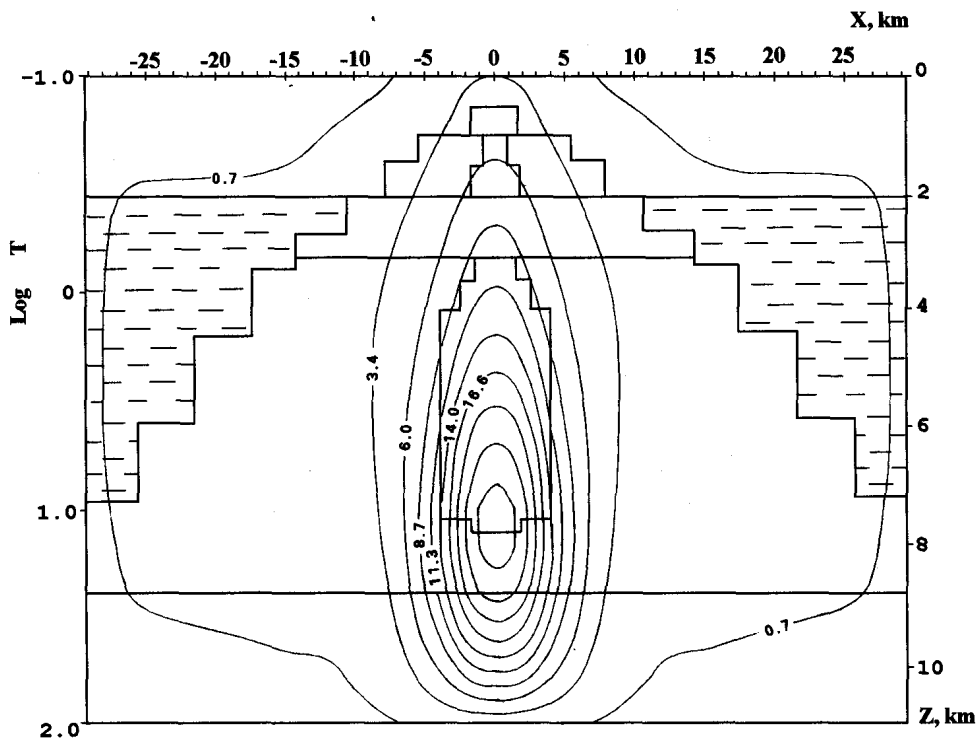


Figure 5. Pseudosection of $\text{Im } E_y$ ($\times 10^1$) for volcano model shown in Fig. 1. Result is based on an incident electrical field, parallel to y-axis.

actual conductivities, the spatial gradients clearly indicate the location of the magma chamber and of the conductive formation above it. The gradient of ϕ_{det} delineates not only the magma chamber but also the flanks of the volcano (Fig. 3). This result matches the findings of Park and Torres-Verdin (1988) and Zhdanov and Spichak (1992) from the interpretation of the phases in array MT data.

Transforms of the in-phase and quadrature parts of the horizontal electrical-field component parallel to the incident electrical field are even more sensitive to gradients of conductivity. Figure 4 shows the vertical cross-section of the model overlapped by the map of the isolines of the $\text{Re } E_y$ transformation. The bunching of isolines correlates with gradients of the conductivity; the local extrema mark upper and lower edges of the magma chamber.

Isolines of the transformations of $\text{Im } E_y$ are shown in Fig. 5. There is strong extremum located at the lower boundary of the magma chamber. No other features related to the model are visible.

Construction of the 3-D pseudostructures from transforms of the in-phase and quadrature parts of the horizontal electrical field and from the impedance phases appears to be a useful tool for delineating the geometric parameters of the complex volcanic environments. The analytical findings of Szarka and Fischer (1989), explaining the behavior of the MT field transformations at the Earth's surface in terms of the distribution of subsurface currents, support this conclusion.

Calculation of the quantities used above can be difficult in practice. One approach might be the analytical continuation of the EM fields, measured at the relief surface S , by means of the well-known integral transformation [see, e.g., Zhdanov (1988)],

$$\mathbf{F}(\mathbf{r}) = \iint_S \{ (\mathbf{n} \cdot \mathbf{F}) \nabla' G + [\mathbf{n} \times \mathbf{F}] \times \nabla' G \} ds' \quad (10)$$

where \mathbf{F} could be \mathbf{E} or \mathbf{H} ; $G = (1/4\pi |\mathbf{r} - \mathbf{r}'|)$ is a Green's function of a free space;

surface S covers all sites, in which the measurements were made; and \mathbf{n} is a unit normal to the surface pointing to the atmosphere.

Depending on the MT field components measured at the surface of the volcano, different integral transformations (Zhdanov, 1988) could be used to convert the field data into the appropriate horizontal electrical-field transform at the artificial plane. The numerical calculations required are rather straightforward and stable, and so, the use of this approach should not cause any problems.

Another important item to be mentioned concerns the selection of the appropriate height of the reference plane. From many experiments with the models of volcanoes, I found that the best height is 250-500 m above the summit. At lower heights, the pseudo-sections become distorted mostly by the nearest parts of the topography and by noise (natural and artificial), whereas at greater heights, details in geoelectrical structure may be lost. Choice of the ideal height for a given structure requires further investigations.

Conclusions

Synthetic MT fields and their transforms, calculated for a 3-D model of a volcano of Hawaiian type, indicate that the phases of the impedance and the in-phase and quadrature parts of the electrical-field components are the most sensitive to the structure (the latter being the most informative in TE mode).

Good qualitative images of the internal structure of the volcano were obtained by transforming the data on a reference plane located slightly higher than the summit of the volcano. The MT fields measured at the Earth's surface could be mapped to this plane by continuation upward. It also might be possible to measure the field components directly in the air, which would allow MT sounding of regions difficult to access by land.

Acknowledgments

The author is thankful to M-me Genevieve Roche and Mrs. Tilda Fleischhacker for kind assistance during preparation of this manuscript.

References

- Fitterman, D. V., Stanley, W. D., and Bisdorf, R. J., 1988, Electrical structure of Newberry Volcano, Oregon: *J. Geophys. Res.*, **93**, 10119-10134.
- Jackson, D. B., and Keller, G. V., 1972, An electromagnetic sounding survey of the summit of Kilauea Volcano, Hawaii: *J. Geophys. Res.*, **77**, 4957-4965.
- Mogi, T., and Nakama, K., 1990, Three-dimensional geoelectrical structure of geothermal system in Kuju volcano and its interpretation: *Geoth. Res. Council Trans.*, **14**, 1513-1515.
- Moroz, Y. R., Kobzova, V. I., Moroz, I. P., and Senchina, A. R., 1988, Analogue modeling of MT-fields of volcano: *Vulkanologiya i seismologiya*, 3,98-104 (in Russian).
- Newman, G. A., Wannamaker, R E., and Hohmann, G. W., 1985, On the detectability of crustal magma chambers using the magnetotelluric method: *Geophysics*, **50**, 1136-1143.
- Park, S. K., and Torres-Verdin, C., 1988, A systematic approach to the interpretation of magnetotelluric data in volcanic environments with applications to the quest for magma in Long Valley, California: *J. Geophys. Res.*, **93**, 13265-13283.
- Spichak, V. V., 1983a, Mathematical modeling of EM-fields in the 3D inhomogeneous media: Ph.D. thesis, IZMIRAN, 1983.
- 1983b, The program package FDM3D for numerical modeling of the three-dimensional electromagnetic fields, *in* Algorithms and programs for solution of the direct and inverse problems of electromagnetic induction in the Earth, Ed. Zhdanov, M., IZMIRAN, 58-68 (in Russian).
- 1985, Differential boundary conditions for the electrical and magnetic fields in the unbounded conducting medium, *in* Electromagnetic sounding of the Earth, Ed. Zhdanov, M., IZMIRAN, 13-22 (in Russian).
- 1990, EM-field transformations and their use in interpretation: *Surv. Geophys.*, **11**, 271-301.
- Szarka, L., and Fischer, G., 1989, Electromagnetic parameters at the surface of conductive halfspace in terms of the subsurface current distribution: *Geophys. Trans.*, **35**, 157-172.
- Zhdanov, M. S., 1988, *Integral transforms in geophysics*: Springer-Verlag.
- Zhdanov, M. S., and Spichak, V. V., 1989, Computer simulation of three-dimensional quasi-stationary electromagnetic fields in geoelectrics: *Dokl. AN USSR*, **309**, 57-60 (in Russian).
- 1992, Mathematical modeling of electromagnetic fields in three-dimensional inhomogeneous media: Nauka Publ. (in Russian).